Postnatally Induced Inactivation of gp130 in Mice Results in Neurological, Cardiac, Hematopoietic, Immunological, Hepatic, and Pulmonary Defects

By Ulrich A.K. Betz,* Wilhelm Bloch,‡ Maries van den Broek,§ Kanji Yoshida,‖ Tetsuya Taga,** Tadamitsu Kishimoto,¶ Klaus Addicks,‡ Klaus Rajewsky,* and Werner Müller*

*From the *Institute for Genetics and the ‡Institute for Anatomy I, University of Cologne, D-50931 Cologne, Germany; the §Institute for Experimental Immunology, University of Zürich, CH-8093 Zürich, Switzerland; the ‖Department of Molecular Immunology, Research Institute for Microbial Diseases, and the ¶Department of Medicine III, Medical School, Osaka University, Osaka 565, Japan; and the **Department of Molecular Cell Biology, Medical Research Institute, Tokyo Medical and Dental University, Tokyo 101, Japan*

Summary

The pleiotrophic but overlapping functions of the cytokine family that includes interleukin (IL)-6, IL-11, leukemia inhibitory factor, oncostatin M, ciliary neurotrophic factor, and cardiotrophin 1 are mediated by the cytokine receptor subunit gp130 as the common signal transducer. Although mice lacking individual members of this family display only mild phenotypes, animals lacking gp130 are not viable. To assess the collective role of this cytokine family, we inducibly inactivated gp130 via Cre-loxP–mediated recombination in vivo. Such conditional mutant mice exhibited neurological, cardiac, hematopoietic, immunological, hepatic, and pulmonary defects, demonstrating the widespread importance of gp130-dependent cytokines.

Key words: gene targeting • conditional gene targeting • Cre/loxP technology • gp130-dependent cytokines • gp130

The cytokine network contains various cytokine families whose members share a common subunit in their receptor complexes (1). One family of cytokines, comprising IL-6, IL-11, leukemia inhibitory factor (LIF),[1] oncostatin M (OSM), ciliary neurotrophic factor (CNTF), and cardiotrophin 1 (CT-1), share the common signal transducer gp130 in their receptors. Individual components of these cytokine receptor complexes are IL-6Rα, IL-11Rα, CNTFRα, CT-1Rα, LIFR, and OSMR. Signal transduction after ligand binding is elicited by homodimerization of gp130 in the case of IL-6 and IL-11, by heterodimerization of gp130 and LIFR in the case of LIF, CNTF, and CT-1, or by heterodimerization of gp130 and OSMR in the case of OSM (2, 3). Thereby, the Janus kinase/signal transducer and activator of transcription (JAK/STAT) pathway (JAK1/JAK2/TYK2 and STAT1/STAT3/STAT5B) and the RAS/mitogen-activated protein kinase (RAS-MAPK) pathway are activated (2).

Mice lacking individual components of this cytokine family or their receptors (IL-6, LIF, CNTF, or IL-11Rα) displayed milder phenotypes than expected. This is most likely due to the redundancy of gp130-dependent cytokines (4–7). The only phenotype exhibited by mice lacking IL-11Rα is female sterility (7, 8). IL-6–deficient animals exhibit defects in hematopoiesis (9), antigen-specific antibody production (except IgM; 4, 10), neutrophilia after infection (11, 12), T_H1 development (12, 13), chemokine induction and leukocyte recruitment (14), acute phase protein (APP) synthesis (4, 15), hepatocyte regeneration (16), fever response (17), neuroglial activation (18), and bone maintenance (19) and display an increased susceptibility to infections with viral, bacterial, fungal, and protozoan pathogens (4, 11–13). LIF-deficient animals exhibit female sterility due to defective blastocyst implantation, postnatal growth retardation, and defects in hematopoiesis and thymocyte proliferation (5, 20).

Not surprisingly, when receptor components used by several members of the gp130 family are inactivated, the consequences are more severe. Thus, mutant animals lacking LIFR, a shared component of the receptor complexes

[1]*Abbreviations used in this paper:* APP, acute phase protein(s); CNTF, ciliary neurotrophic factor; CT-1, cardiotrophin 1; JAK, Janus kinase; LIF, leukemia inhibitory factor; MAPK, mitogen-activated protein kinase; OSM, oncostatin M; s, soluble; SAP, serum amyloid *P*; STAT, signal transducer and activator of transcription; VSV, vesicular stomatitis virus.

J. Exp. Med. © The Rockefeller University Press • 0022-1007/98/11/1955/11 $2.00
Volume 188, Number 10, November 16, 1998 1955–1965
http://www.jem.org

for LIF, CNTF, and CT-1, are not viable and die perinatally, exhibiting placental, skeletal, neural, and metabolic defects as well as a loss of motor neurons (21, 22). Although CNTF-deficient mice are only marginally affected by a gradual loss of motor neurons, animals lacking CNTFRα die postnatally (6, 23), suggesting that the CNTFRα has more than one ligand. Animals deficient for the common signal transducer gp130 die after day 12.5 postconception or postnatally, depending on the genetic background (24, 25). These embryos exhibit growth retardation, decreased hematopoiesis in the fetal liver, and reduced numbers of primordial germ cells. In addition, they also show a disrupted placental architecture, a hypoplastic ventricular myocardium, and an increased number of osteoclasts (24, 25).

Due to the redundancy of gp130-activating cytokines on one hand and premature lethality of animals lacking shared receptor components on the other, it has so far been impossible to assess the collective physiological role of gp130-dependent cytokines in the adult animal. To answer this question, we inactivated the common signal transducer gp130 inducibly by conditional gene targeting after postnatal lethality had been bypassed (26).

Materials and Methods

Mice

C57BL/6 mice were obtained from Charles River GmbH (Sulzfeld, Germany), and IL-6–deficient mice were provided by H. Mossmann (MPI für Immunologie, Freiburg, Germany). All animals were kept under standard conditions and maintained on acidified water.

Flow Cytometry

Staining was done with fluorochrome (FITC, PE, or Cy-Chrome) or biotin-conjugated mAbs for flow cytometric analysis on a FACScan® (Becton Dickinson, Mountain View, CA). Biotin-conjugated mAb was detected using streptavidin-PE (Southern Biotechnology Associates, Inc., Birmingham, AL). mAb specific for gp130 (RX187) was a gift from K.-I. Akamatsu (Chugai Pharmaceutical Co. Ltd., Tokyo, Japan). mAbs were purchased from PharMingen (San Diego, CA) or Serotec Ltd. (Oxford, UK).

Hematologic Analysis

Blood was taken from mouse tail vein, diluted with PBS, and leukocyte, erythrocyte, and thrombocyte counts were determined by cell counter (model STKS; Coulter Corp., Hialeah, FL). GM-CFU were measured using methylcellulose medium supplemented with recombinant cytokines (Methocult GF M3434; CellSystems, Biotechnologie Vertrieb GmbH, Remagen, Germany) according to the manufacturer's instructions.

Soluble gp130 ELISA

The concentration of soluble gp130 (sgp130) in the blood was determined using a sandwiched ELISA. Plates were coated with anti-gp130 mAb (RX435) to capture sgp130 from the mouse serum. The presence of bound sgp130 was detected with biotinylated anti-gp130 antibody (RX187 [27]) followed by streptavidin-conjugated alkaline phosphatase (Boehringer Mannheim, Mannheim, Germany). Recombinant sgp130 was used as a standard.

Measurement of Acute Phase Response after LPS Injection

Mice were injected intraperitoneally with 1 mg LPS purified from *Escherichia coli* (Sigma, Deisenhofen, Germany) per kg body wt. Hematic glucose was measured using a Glucometer 3 (Bayer

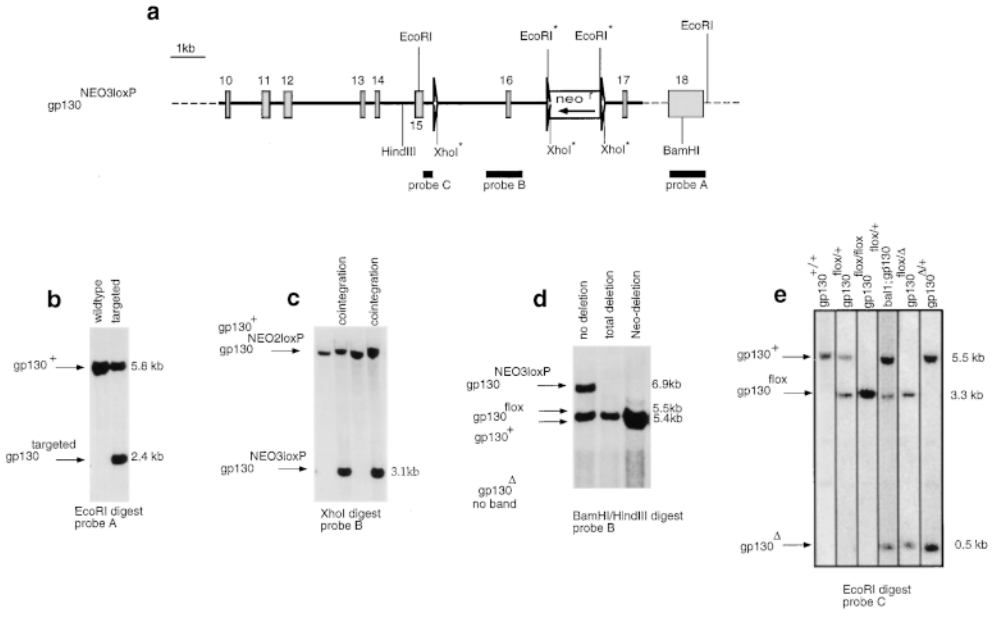

Figure 1. Gene targeting. (*a*) Gene targeting vector (**bold line**) homologously recombined into the gp130 locus (*dashed line*), thereby generating the targeted allele gp130^{NEO3loxP}. Exon sequences (*rectangles*); loxP sites (*triangles*). The transcriptional orientation of the neomycin resistance gene is shown. Restriction sites used for Southern analysis are given; those marked with an asterisk are not present in the wild-type locus but are introduced via the targeting vector. The probes used for Southern analysis are shown (*black*). In the gp130^{NEO2loxP} allele, the loxP site upstream of exon 16 is missing due to lack of cointegration. (*b*) Southern analysis to identify homologous recombinant clones. The size and position of the bands representing the gp130^{+} (wild-type) and gp130^{targeted} (gp130^{NEO2loxP} or gp130^{NEO3loxP}) alleles are given. (*c*) Southern analysis to identify clones harboring a cointegrated upstream loxP site. The position and size of the bands representing the gp130^{NEO2loxP} and gp130^{+} alleles or the gp130^{NEO3loxP} allele are given. (*d*) Southern analysis to identify clones which have deleted the neomycin resistance gene but not exon 16 after transient expression of Cre-recombinase. The position and size of the bands representing the gp130^{+}, gp130^{flox}, and gp130^{NEO3loxP} alleles are given. (*e*) Southern blot prepared with mouse tail DNA in order to genotype the animals. The position and size of the bands representing the gp130^{+}, gp130^{flox}, and gp130$^{\Delta}$ alleles are shown. Lane *4*: *bal1*, Cre-transgenic (reference 31).

Diagnostic GmbH, München, Germany). The concentration of serum amyloid *P* (SAP) and C3 in the serum was measured by ELISA using sheep anti–mouse SAP antiserum (Calbiochem Novabiochem GmbH, Bad Soden, Germany), rabbit anti–mouse SAP antiserum (Calbiochem Novabiochem GmbH), alkaline phosphatase–conjugated goat anti–rabbit IgG antiserum (Promega Deutschland GmbH, Mannheim, Germany), goat anti–mouse C3 antiserum (Organon Teknika-Cappel, Durham, NC), and peroxidase-conjugated goat anti–mouse C3 antiserum with a SAP/C3 standard as a reference (Calbiochem Novabiochem GmbH).

Serum Antibody Levels

The concentrations of the different Ig isotypes in the serum were determined by ELISA as described previously (28).

Fixation Procedure

After anesthesia, the lung was perfusion-fixed with 4% paraformaldehyde for 20 min at 15 cm H_2O using an intratracheal catheter. Subsequently, mice were transcardially perfused using the same fixative at a perfusion pressure of 60 cm H_2O for the same time. Organs were removed and fixed for an additional 4 h in the same fixative.

Light and Electron Microscopy

4% paraformaldehyde perfusion-fixed mouse tissue was postfixed with 2% osmium tetroxide in 0.1 M PBS for 2 h at 4°C. After a thorough wash in 0.1 M phosphate buffer for 10 min three times, the slices were dehydrated in a graded ethanol series and infiltrated with and embedded in araldite. Sections of plastic-embedded specimens were cut with a glass or diamond knife on a Reichert ultramicrotome.

Morphometric Study

For quantification of the ventricular wall thickness, a 2-mm slice perpendicular to the heart axis at the upper half of the ventricular region was cut out, divided in four pieces, and measured in five randomly selected parts of both ventricles at two planes. The myocyte width was measured perpendicular to the long axis of the myocyte slice on 60 randomly selected myocytes of each ventricle using Optimas 6.0. Quantification of the binucleated hepatocytes was performed on methylene blue–stained semithin sections of three specimens from different parts of the liver. 100 hepatocytes of 10 randomly selected areas were counted.

Infection Experiments

Vaccinia. Mice were infected intravenously with 2×10^6 PFU vaccinia-WR. Viral titers in the lungs were determined at day 5 after infection by plaquing 10-fold dilutions of tissue homogenates on monolayers of BSC40 cells, followed by crystal violet staining after 48 h.

Vesicular Stomatitis Virus. Mice were infected intravenously with 2×10^6 PFU vesicular stomatitis virus, strain Indiana (VSV-IND). Mice were bled on days 4, 8, 12, and 20 after infection, and VSV-neutralizing Ig and IgG antibodies were determined as described (29). The titer was determined by twofold dilution steps of 1:40 prediluted sera, and reduction of IgM was achieved by treating the sera with 0.1 M 2-ME. Titer is defined as the dilution that reduced the number of plaques to half of the control.

Listeria. Mice were infected intravenously with 3×10^3 CFU *Listeria monocytogenes*. The number of viable bacteria recovered from liver and spleen was determined 5 d after infection by plating 10-fold serial dilutions of organ homogenates on brain–heart infusion agar plates.

Results

Generation of a Mouse Line Allowing for Conditional Inactivation of gp130. A targeting vector was constructed in which the exon encoding the transmembrane region of gp130 was flanked with two loxP sites (Fig. 1 *a*). Homologous recombinant E14 embryonic stem cell colonies were generated (Fig. 1 *b*) which had cointegrated the upstream loxP site (allele: $gp130^{NEO3loxP}$) (Fig. 1 *c*). After transient transfection with the Cre-encoding plasmid pICCre, clones were

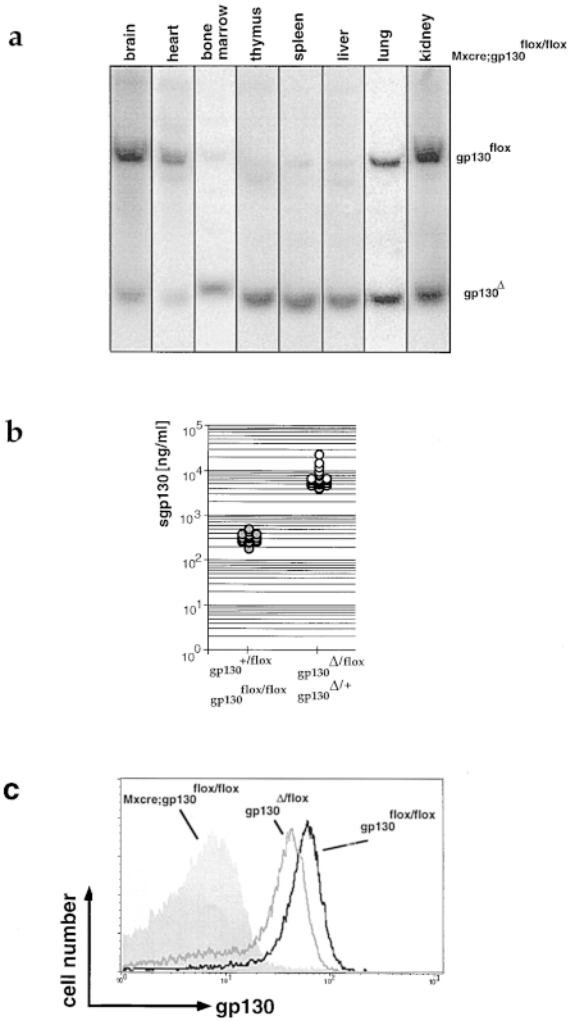

Figure 2. Inactivation of gp130. (*a*) Southern blot prepared with DNA of various organs of an adult Mx-cre;$gp130^{flox/flox}$ mouse injected postnatally with IFN to induce expression of Cre-recombinase. The Southern blot was performed as described in Fig.1 *e*. (*b*) Concentration of sgp130 in the blood of wild-type, heterozygous, or homozygous $gp130^{flox}$ animals (*shaded circles*) and heterozygous $gp130^{\Delta}$ animals (*open circles*) as measured by ELISA. One symbol represents data obtained for one animal. (*c*) Cell surface expression of gp130 on peripheral blood $CD8^+$ T cells of adult $gp130^{flox/flox}$ (*black line*), $gp130^{\Delta/flox}$ (*gray line*), and Mx-cre;$gp130^{flox/flox}$ animals which were injected with IFN as newborns (*gray histogram*).

identified which had deleted neo^r but not the transmembrane exon (Fig. 1 *d* [30]). The resulting allele (gp130^{flox}) can be inactivated by Cre-loxP–mediated recombination (thereby generating gp130$^{\Delta}$) through removal of the transmembrane exon and a resulting frame shift. Embryonic stem cells were injected into C57BL/6 blastocysts. Resulting chimeric mice were crossed with C57BL/6 animals to establish mice carrying the gp130^{flox} mutation in the germ line (Fig. 1 *e*). As mice homozygous for the gp130^{flox} allele were phenotypically indistinguishable from wild-type animals, the introduction of loxP sites apparently did not affect gp130 expression significantly. To inactivate the loxP-flanked allele in the germ line, gp130$^{flox/flox}$ animals were crossed to Bal1 cre-transgenic mice (31).

Inducible Inactivation of gp130. To allow for inducible inactivation of gp130, gp130$^{flox/flox}$ animals were crossed to

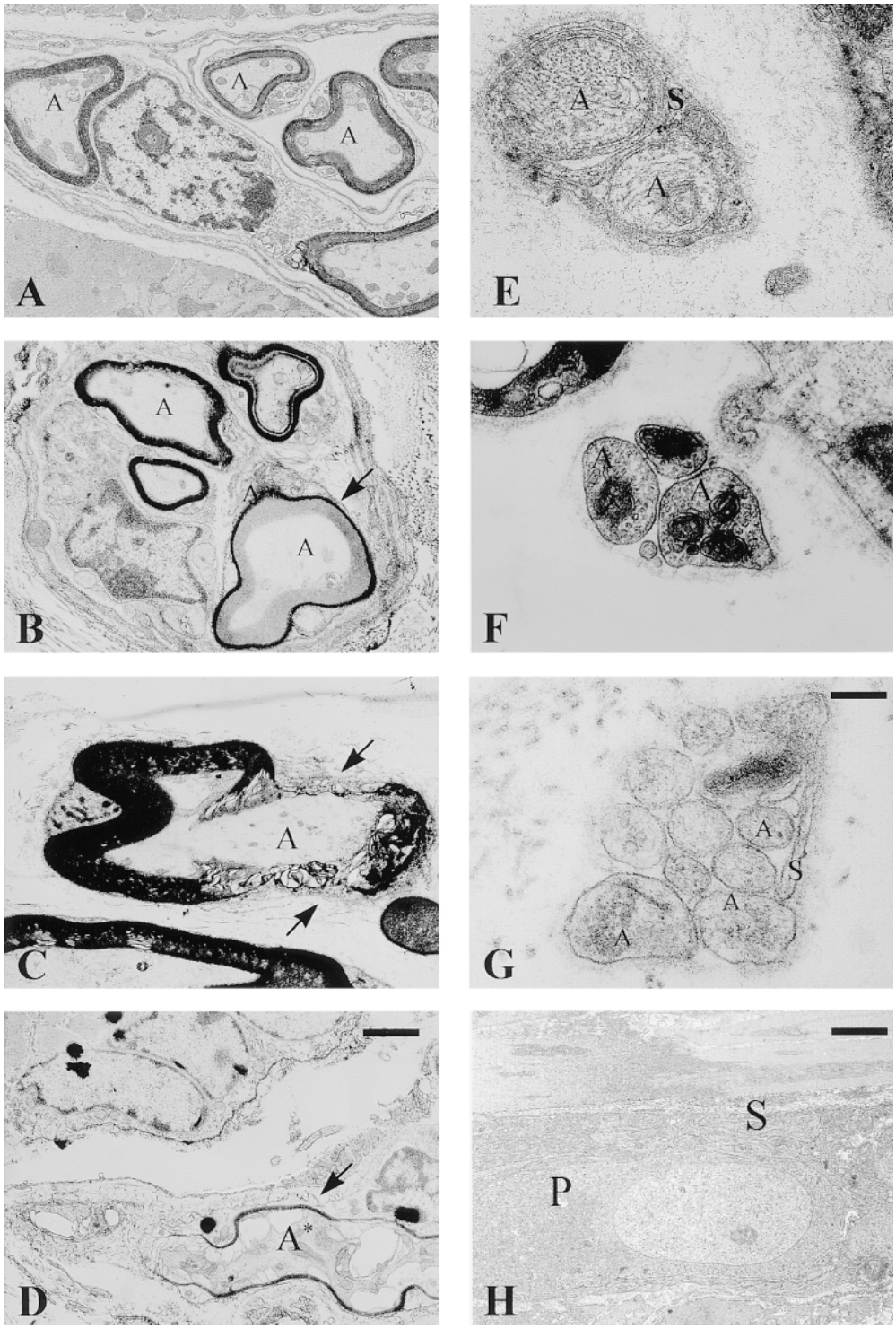

Figure 3. Degeneration of peripheral nerves in conditional gp130-mutant mice. Electron microscopic analysis of peripheral somatic nerves innervating skeletal muscle (*A–D*) and vegetative nerves innervating the heart muscle (*E* and *F*) or gut (*G* and *H*) of control gp130$^{flox/flox}$ (*A* and *E*) and conditional gp130-mutant animals (*B–D*, *F–H*). *A*, Axon; *S*, Schwann cell; *P*, cell body. (*A*) Control, skeletal muscle: the myelinated nerve fibers show a regular myelin and axon structure (*A*). (*B*) Conditional gp130-mutant, skeletal muscle: disappearance of laminar myelin structure (*arrow*) without signs of axon lysis. (*C*) Conditional gp130-mutant, skeletal muscle: in certain areas the myelin sheath shows a complete lysis (*arrow*). (*D*) Conditional gp130-mutant, skeletal muscle: the degeneration of the myelin sheath (*arrow*) is associated with an axon lysis (*A**). (*E*) Control, heart: the axon bundle has a complete and intact Schwann cell covering (*S*). (*F*) Conditional gp130-mutant, heart: the axon bundle (*A*) shows a partial failure of Schwann cell covering, while the basal lamina completely surrounds it. (*G*) Conditional gp130-mutant, gut: also in a thicker axon bundle of the gut an incomplete covering of the axon (*A*) by Schwann cells (*S*) is recognizable. (*H*) Conditional gp130-mutant, gut: the glia (*S*) covering of a myenteric neuron's cell body (*P*) shows no signs of alteration. For *A–D*, bar (in *D*) = 1 μm; for *E–G*, bar (in *G*) = 0.25 μm; for *H*, bar = 1.5 μm.

mice expressing Cre-recombinase under control of the IFN-responsive Mx1 promoter (Mx-cre [32]). 1–3 d after birth, mice were injected with 5×10^6 U IFN-α_2/α_1 to induce Cre-mediated recombination (33). 3–4 wk later, mice were genotyped and tested for the efficiency of Cre-mediated deletion by Southern or FACS® analysis using anti-gp130 antibody (RX187 [27]). Cre-mediated deletion of the loxP-flanked allele was close to completion in hematopoietic cells and in hepatocytes, whereas the extent of deletion varied in other organs between 20 and 70% (Fig. 2 *a*). Possible side effects of IFN-α treatment do not pose a problem for our analysis of the resulting phenotype, as the conditional mutants were compared with control animals that likewise received a postnatal IFN-α injection (34).

The gp130$^{\Delta}$ Allele Is Nonfunctional. As expected from the removal of the transmembrane region, in the blood of animals carrying a gp130$^{\Delta}$ allele, the concentration of sgp130 was 20-fold increased compared with gp130$^{+/+}$ or gp130$^{flox/flox}$ controls (Fig. 2 *b*). In inter-crosses between heterozygous gp130$^{\Delta}$ mice, no viable gp130$^{\Delta/\Delta}$ animals were obtained. gp130$^{\Delta/\Delta}$ embryos could be found up to day 18.5 after conception but were severely reduced in size compared with their wild-type or heterozygous littermates (not shown). As measured by FACS® on T cells, gp130 surface expression was only marginally reduced in gp130$^{\Delta/flox}$ compared with gp130$^{flox/flox}$ mice, whereas cells were gp130^{-} after Cre-mediated recombination in Mx-cre;gp130$^{flox/flox}$ animals (Fig. 2 *c*).

Accordingly, Mx-cre;gp130$^{flox/flox}$ mice treated with IFN-α_2/α_1 as newborns are hereafter referred to as conditional gp130-mutants. These animals exhibited a diverse phenotype, were weight-reduced, and had a reduced life span, with 50% of the animals dying before the age of 5 mo (not shown).

gp130 Deficiency Leads to Schwann Cell Decomposition and Degeneration of Both Myelinated and Unmyelinated Peripheral Nerves. gp130-dependent cytokines have been shown to play an important role in the generation and maintenance of motor neurons (6, 21, 23, 35). Interestingly, in peripheral somatic nerves innervating skeletal leg muscle (musculus gastroceminus), conditional gp130-mutant mice exhibited a degeneration of the myelin sheath (Fig. 3, *A–D*). The defects on the myelin sheath ranged from disappearance of the laminar structure (Fig. 3 *B*) to complete loss of myelin (Fig. 3, *C* and *D*) and axon lysis (Fig. 3 *D*). In myocardium as well as in the gut, Schwann cell covering of some small and thick axon bundles was also incomplete in the conditional mutants (Fig. 3, *F* and *G*). However, in contrast to the axon terminals, most cell bodies showed an unaltered glia covering (Fig. 3 *H*). This result shows that gp130-dependent cytokines in adult animals not only influence the survival of motor neurons, as described in mice deficient for CNTF or CNTF/LIF, but also affect Schwann cell covering in myelinated and unmyelinated peripheral nerves.

Myocardial Abnormalities in Conditional gp130-mutant Mice. Although the efficiency of Cre-mediated recombination in the heart was low (20–30%; see also Fig. 2 *a*), distinct morphological alterations were apparent. In the cardiac ventricles of conditional mutant animals, a subpopulation of cardiomyocytes exhibiting a reduction in diameter was detectable. In the left ventricle, for example, 16% of the myocytes from conditional gp130-mutant animals showed a diameter <10 μm, compared with only 2.8% in controls. In addition, conditional gp130-mutants exhibited a thinning of the left (from 792 ± 149 to 619 ± 101 μm) and right (from 344 ± 56 to 248 ± 48 μm) ventricular wall of the heart, and in some cases right ventricular dila-

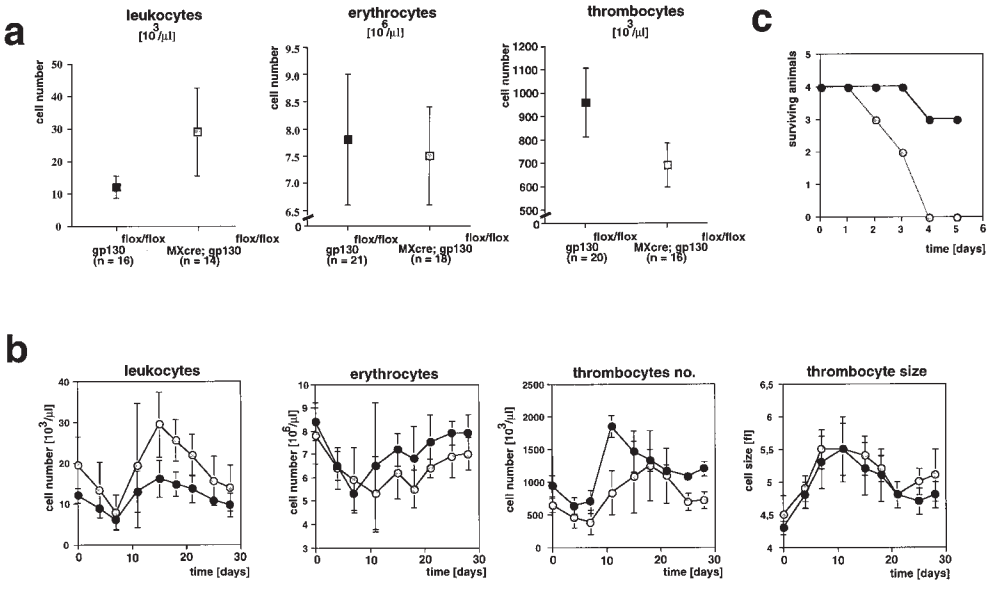

Figure 4. Hematopoietic defects in the absence of functional gp130. Conditional gp130-mutant (*shaded symbols*); gp130$^{flox/flox}$ (*filled symbols*). (*a*) Basal hematology profile. The number of leukocytes, erythrocytes, and thrombocytes was determined in blood collected from the tail vein. (*b*) Recovery after 5-FU–induced hematopoietic ablation. The kinetics of recovery of leukocytes, erythrocytes, and thrombocytes in the peripheral blood after a single intraperitoneal administration of 150 mg/kg 5-FU at day 0 was determined over a period of 30 d ($n = 7$ for each genotype). (*c*) Survival after immune thrombocytopenia. Thrombocytopenia was induced by intraperitoneal injection of 3 μl adsorbed rabbit anti–mouse platelet serum (Inter-Cell Technologies, Inc., Hopewell, NJ) diluted in PBS at day 0, and survival of animals was subsequently monitored.

tion (not shown). As a cardiac defect was also detected in the conventional gp130-deficient embryos (24), this result shows that gp130-dependent cytokines affect cardiomyocyte proliferation or maintenance beyond embryonic development.

Defects in Hematopoiesis in the Absence of gp130-mediated Signals. An influence of gp130-dependent cytokines on hematopoiesis is well established. It was also apparent in mice deficient for IL-6 or LIF, although numbers of circulating white and red blood cells and thrombocytes were still normal (9, 20). In contrast, conditional gp130-mutant mice displayed a reduction in thrombocyte count in the peripheral blood together with an increased number of circulating leukocytes, which is unexplained at the moment. Red blood cell counts were normal (Fig. 4 *a*). To further assess the role of gp130 in hematopoiesis, we abrogated hematopoiesis by 5-fluoro-5′-deoxyuridine (5-FU) treatment, which kills cycling cells (Fig. 4 *b*), and determined the ability of the mutant mice to recover. Although leukocytes were generated efficiently in the conditional gp130-mutant animals, resynthesis of erythrocytes and thrombocytes was impaired. A defect in thrombocyte synthesis in the conditional gp130-mutant animals was also apparent after induction of thrombocytopenia by administration of antithrombocyte antiserum, which could not be compensated for by the mutant animals (Fig. 4 *c*).

The number of hematopoietic precursors (CFU-S, GM-CFU) was reduced by 40% in the bone marrow of conditional mutants, whereas in the spleen a twofold increased number of GM-CFU could be detected (not shown). However, the reduction in hematopoietic precursors was more dramatic in gp130-deficient embryos (24).

Accordingly, gp130-dependent cytokines seem to be critically important for establishing the hematopoietic compartment during embryogenesis or after hematopoietic ablation. Under steady state conditions, they continue to play a major role in thrombopoiesis.

IL-6 Is the Principal Member of gp130-dependent Cytokines in the Immune System. In accordance with what is seen in IL-6–deficient mice (4), T cell content in conditional gp130-mutant animals was reduced by 30%, whereas B cell development was not affected. Although IL-6 has been considered to be essential for the terminal differentiation of B cells into Ig-secreting plasma cells (36), mice lacking IL-6 surprisingly displayed normal total serum antibody levels (4). Likewise, in conditional gp130-mutants, no general defect in antibody production could be detected and antibody levels were not reduced compared with controls (Fig. 5). However, the mutants exhibited increased levels of IgG1 and IgE in the blood, indicative for increased IL-4 production, as demonstrated previously in the IL-2–deficient mouse mutant (37).

To directly compare the ability of IL-6–deficient and conditional gp130-mutant mice to control infections with viral and bacterial pathogens, we infected animals with VSV, vaccinia virus, and *L. monocytogenes*. During VSV infection, production of virus-neutralizing IgG was reduced by three- to fourfold in conditional gp130-mutant animals, as in IL-6–deficient mice (Fig. 6 *a*), whereas no significant difference in neutralizing IgM level was detected (Fig. 6 *b*). Infection with the cytopathic vaccinia virus is controlled by the soluble mediators IFN-γ and TNF-α, rather than cytotoxic T cells (38–40). 5 d after infection with vaccinia vi-

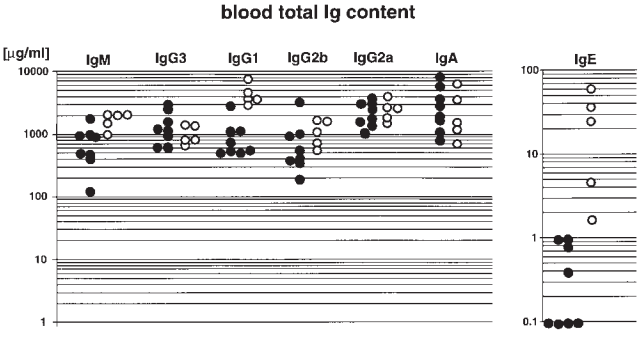

Figure 5. Antibody production in conditional gp130-mutant animals. Levels of different Ig isotypes in 12–15-wk-old conditional gp130-mutant (*open circles*) and gp130$^{flox/flox}$ animals (*filled circles*) as quantitated by ELISA. One symbol represents data obtained for one animal.

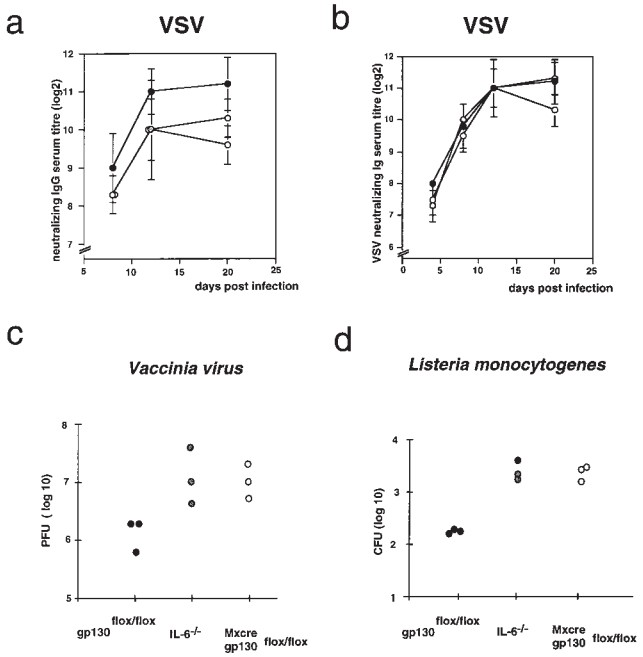

Figure 6. Increased susceptibility to viral and bacterial infections of conditional gp130-mutant animals. (*a* and *b*) The anti-VSV IgG (*a*) and IgM (*b*) response after infection was determined as described in Materials and Methods in conditional gp130-mutant (*open circles*), IL-6–deficient (*shaded circles*), and gp130$^{flox/flox}$ (*filled circles*) control animals (at least three per group and time point). (*c*) The number of vaccinia virus recovered from lung at day 5 after infection (see Materials and Methods) was determined in conditional gp130-mutant (*open circles*), IL-6–deficient (*shaded circles*), and gp130$^{flox/flox}$ (*filled circles*) control animals. One symbol represents data obtained from one mouse. (*d*) The number of viable *L. monocytogenes* in the spleen 5 d after infection (see Materials and Methods) was determined in conditional gp130-mutant (*open circles*), IL-6–deficient (*shaded circles*), and gp130$^{flox/flox}$ (*filled circles*) control animals. One symbol represents data obtained from one mouse.

rus, viral titers in the lung were increased by a factor of 10–30 in conditional gp130-mutant and IL-6–deficient mice compared with $gp130^{flox/flox}$ controls (Fig. 6 *c*). Infections with *L. monocytogenes* are controlled by neutrophilic granulocytes and macrophages and cleared by a T cell–dependent mechanism (41). Also in this case, the pathogen titer was increased 10–20-fold in spleen (Fig. 6 *d*) of conditional gp130-deficient animals 5 d after infection, again as observed in IL-6–deficient mice.

In summary, the immune system of gp130-deficient animals does not seem to be more severely affected than it is in IL-6–deficient animals. Thus, our data suggest that IL-6 is the principal member of the gp130-dependent cytokine family with regard to immune function.

Morphologic Abnormalities in the gp130-mutant Liver Are Accompanied by a Decreased Ability to Synthesize APP. gp130-dependent cytokines have been reported to play a major role in liver regeneration and APP synthesis (4, 15, 16, 42). gp130-mutant livers exhibited a decreased content of binucleated hepatocytes (12.2% compared with 21.4% in controls). Further signs of liver abnormalities in the mutant animals (Fig. 7) were an increased number of Kupffer cells, a scarce content of rough and smooth endoplasmic reticulum, an increase of lipid vacuoles, an increase of laminar bodies, a widening of the Disse space and intercellular space between hepatocytes, dense clustering of mitochondria, reduction and morphological alteration of microvilli, and a shift in glycogen particles from the rosette α to the monoparticulate β form. However, mitochondria and bile canaliculi were indistinguishable in mutant and wild-type liver. In older mice, part of the gp130-mutant liver tissue was replaced by fibrotic tissue (Fig. 7, *C* and *D*).

These drastic morphological changes were reflected by a severely decreased ability to synthesize APP. 24 h after intraperitoneal injection of LPS, control animals displayed a considerable increase in the concentration of the APP SAP and

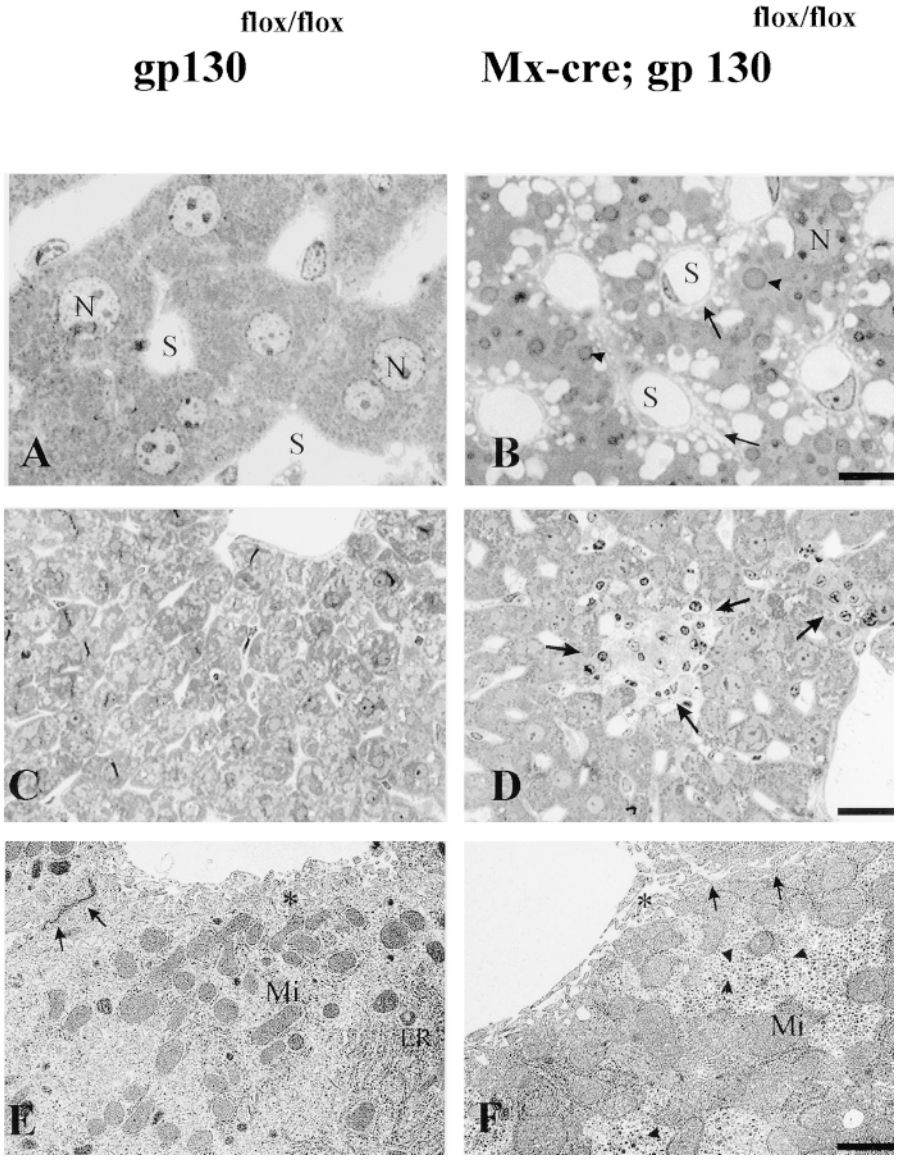

Figure 7. Hepatic abnormalities in the conditional mutants. Light (*A–D*) and electron (*E* and *F*) microscopic analysis of control (*A*, *C*, and *E*) and gp130-mutant (*B*, *D*, and *F*) liver. *N*, Nucleus; *S*, liver sinus. After 6 wk, gp130-mutant liver (*B*) has a high amount of lipid droplets (*arrowheads*), widening of the Disse and intercellular space (*arrows*), a reduced content of binucleated hepatocytes, and an increase in Kupffer cells compared with controls (*A*). In 12-mo-old gp130-mutant liver, a part of the liver parenchyma is replaced by fibrotic material (*D*, *arrows*), a phenomenon not observed in the $gp130^{flox/flox}$ control animals (*C*). The ultrastructure of gp130-mutant liver (*F*) gives evidence for a rarification of smooth and rough endoplasmic reticulum (*ER*), a dense clustering of mitochondrial (*Mi*) and monoparticulate (β) glycogen granules (*triangle*), a decrease of microvilli (*), and an enlargement of Disse and intercellular spaces (*arrows*) compared with the $gp130^{flox/flox}$ control (*E*). For *A* and *B*, bar = 5 μm; for *C* and *D*, bar = 20 μm; for *E* and *F*, bar = 0.5 μm.

complement C3 in the blood. Yet, the conditional gp130-mutant animals failed to do so (Fig. 8 *a*). Monitoring SAP and blood glucose levels revealed that this was not simply due to a delay in APP synthesis in the mutants (Fig. 8 *b*).

Conditional gp130-mutant Mice Develop Emphysema with Increasing Age. Investigation of the lungs revealed the development of emphysema with increasing age in the conditional gp130-mutant animals. At the age of 6 wk, no sign of emphysema formation or elastin degradation was observable (not shown). Although after 5 mo only a scarce alteration of lung morphology could be observed on methylene blue–stained sections of the mutants, there was a distinct reduction of elastic fibers, as demonstrated by orcein staining (Fig. 9, *A* and *B*). However, at the age of 12 mo, a distinct emphysema could be observed in the conditional gp130-mutants, which exhibited an enlargement of the acinus and destruction of respiratory tissue associated with fibrosis (Fig. 9, *C* and *D*). Thus, the mutant animals displayed a time-dependent reduction of elastic fibers, followed by the development of lung emphysema, a phenotype unprecedented in the available mutant mice lacking individual components of the gp130–cytokine system.

Discussion

Degeneration of Peripheral Nerves in the Absence of gp130-mediated Signals. The progressive degeneration of peripheral nerves starting with Schwann cell degradation (Fig. 3) cannot be explained by an inflammatory process due to increased pathogen susceptibility of gp130-mutant animals, as the tissue surrounding the damaged nerves did not show any morphologic alterations and the defects are uniform in peripheral vegetative nerve systems, in myocardic and enteric systems, and in somatic nerves in skeleton muscle. As no Schwann cell defect has been described to date in conjunction with the motor neuron deficits of CNTF- or LIF/CNTF-deficient mice (6, 35), it is conceivable that an as yet uncloned ligand is the main mediator for gp130 signals on Schwann cells. Alternatively, the observed defect may become apparent only after simultaneous inactivation of several gp130-dependent cytokines, as various family members have been reported to enhance the survival of oligodendrocytes in vitro (43).

gp130 Signals Are Important for Thrombopoiesis. The analysis presented here points to a special importance of gp130-dependent cytokines for the synthesis of thrombocytes, as already under steady state conditions thrombocyte number was reduced in the absence of functional gp130 (Fig. 4). It has been shown previously that IL-6, IL-11, LIF, OSM, IL-3, and thrombopoietin can increase platelet production (44). In addition, IL-6 transgenic mice showed an increase in the number of mature multinuclear megakaryocytes in the bone marrow (45). Nevertheless, neither IL-6–, IL-11R–, nor LIF-deficient mice displayed decreased platelet counts, although IL-6–deficient mice had lower numbers of CFU-MK (9). The redundant function of gp130-dependent cytokines with regard to thrombocyte production is reflected by the fact that inactivation of gp130 produced a more severe phenotype than inactivation of any single ligand.

Redundancy among Different gp130-dependent Cytokines Does Not Play a Major Role in the Immune System. The effects of gp130 deficiency in the immune system do not seem to be more severe than those caused by the absence of IL-6 alone, as judged by T cell numbers, total Ig content in the blood (Fig. 5), antigen-specific antibody production, and susceptibility to infection by viral and bacterial pathogens (Fig. 6). This argues against a major regulatory role of gp130-dependent cytokines in the immune system apart from IL-6, indicating that redundancy among different family members is not widespread in the regulation of immunity. Also, gp130 inactivation was very efficient; in hematopoietic cells, the possibility exists that remaining wild-type cells were selected during immune responses, thereby attenuating the phenotype displayed by the conditional mutants.

gp130 Plays a Major Role in the Acute Phase Response and Lung Physiology. The importance of IL-6 for hepatocytes has only been apparent under stress conditions, e.g, provoked by localized tissue damage or partial hepatectomy (4, 15, 16). In contrast, in the absence of gp130, profound histological changes arose spontaneously in the liver (Fig. 7). Likewise, although APP production after injection of LPS was almost normal in IL-6–deficient mice (4, 15), in gp130-

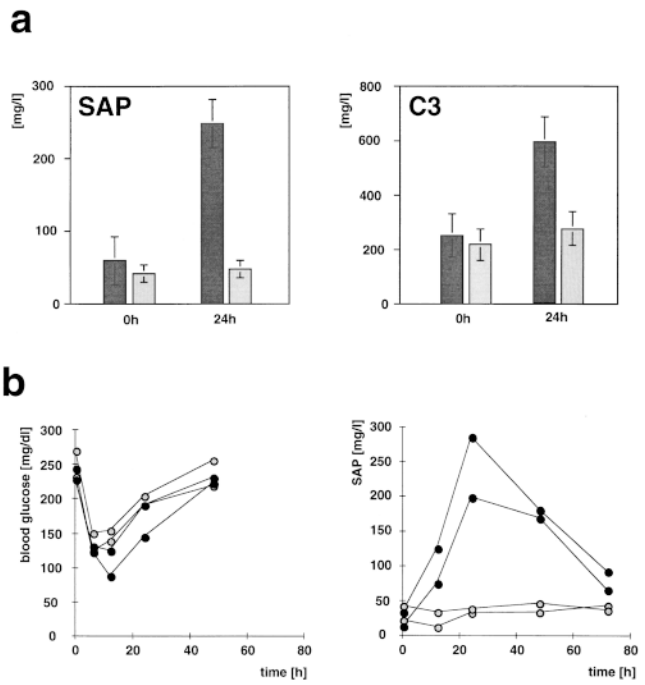

Figure 8. No increased synthesis of APP in the absence of functional gp130. (*a*) Conditional gp130-mutant (*gray bars*, $n = 5$) and $gp130^{flox/flox}$ control mice (*black bars*, $n = 5$) were injected intraperitoneally with 1 mg/kg LPS, and the concentration of the APP SAP and C3 in the serum was measured 24 h later by ELISA. (*b*) The hematic glucose and serum SAP concentrations were monitored over a period of 80 h after challenge with 1 mg/kg LPS in gp130-mutant (*shaded symbols*) and control (*filled symbols*) animals.

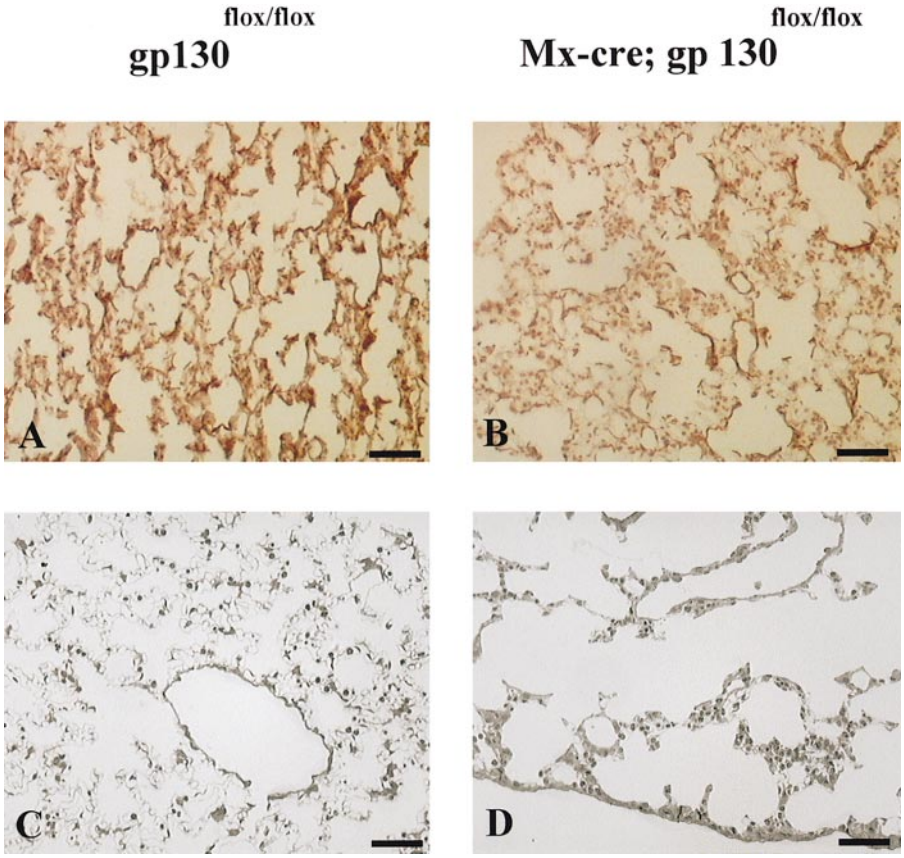

Figure 9. Emphysema development in conditional gp130-mutant animals. Representative histological appearance of lungs from different ages of $gp130^{flox/flox}$ and conditional gp130-mutant mice. (*A* and *B*) Orcein staining. After 5 mo of age, conditional gp130-mutants (*B*) showed a distinct reduction of elastic fibers (*red*) compared with controls (*A*). (*C* and *D*) Methylene blue staining. At the age of 12 mo, a distinct rarification of alveolar walls was detectable in the absence of functional gp130 (*D*) compared with $gp130^{flox/flox}$ controls (*C*). Bar = 60 μm.

mutant mice no increased synthesis of APP could be detected (Fig. 8). This could reflect a specific role of gp130-dependent cytokines other than IL-6 in the induction of APP synthesis or a general synthetic deficiency of gp130-deficient hepatocytes, which exhibit drastic morphological alterations including an underdeveloped endoplasmic reticulum.

Conditional gp130-mutant animals developed emphysema with increasing age, starting with elastic fiber degradation (Fig. 9). If neutrophil elastase activity during infections cannot be efficiently held in check by antiproteases, which are a major component of the APP, elastin digestion and finally emphysema development results (46). Accordingly, humans suffering from congenital α_1-antitrypsin deficiency suffer from emphysema with increasing age (47). In this regard, it is interesting to note that apart from hepatocytes, lung epithelial cells are also a source of antiproteases. Here synthesis can be stimulated by OSM, but not by other gp130-dependent cytokines (47, 48). This predicts that OSM-deficient or OSM/IL-6 double mutant animals may likewise suffer from emphysema development.

Concluding Remarks. Taken together, we were able to assess the function of gp130 by ablating the common signal transducer gp130 in mice after birth. The observed demyelination of peripheral nerves, thrombocytopenia, the disrupted liver architecture in combination with an impaired acute phase response, and the formation of emphysema in the lung did not occur in animals lacking individual members of the gp130-dependent cytokine family generated to date. Thus, either these effects become apparent only when several gp130-dependent cytokines have been inactivated simultaneously or they are due to uncharacterized family members. The diverse phenotype of conditional gp130-mutant animals demonstrates the widespread importance of gp130-dependent cytokines, and points to their potential therapeutic use in conditions such as emphysema formation, thrombocytopenia, and nerve degeneration.

We thank K.-I. Akamatsu (Chugai Pharmaceutical Co. Ltd., Tokyo, Japan) for anti-gp130 antibody (RX187), C. Weissmann for recombinant IFN-α_2/α_1, V. Poli for ELISA protocols, M. Kopf and H. Mossmann for IL-6–deficient animals, and R. Zinkernagel and L. Pao for reading the manuscript.

This work was supported by the Bundesministerium für Bildung, Wissenschaft, Forschung und Technologie, Förderkennzeichen 01 KS 9502 (Zentrum für Molekularbiologische Medizin Köln [ZMMK], Cologne).

Address correspondence to Werner Müller, Institute for Genetics, Weyertal 121, D-50931 Cologne, Germany. Fax: 49-221-470-5185; E-mail: w.mueller@uni-koeln.de

U.A.K. Betz's present address is Pharma Research Antiinfectives, Bayer AG, D-42096 Wuppertal, Germany.

Received for publication 13 August 1998.

References

1. Kishimoto, T., T. Taga, and S. Akira. 1994. Cytokine signal transduction. *Cell*. 76:253–262.
2. Taga, T., and T. Kishimoto. 1997. Gp130 and the interleukin-6 family of cytokines. *Annu. Rev. Immunol*. 15:797–819.
3. Ichihara, M., T. Hara, H. Kim, T. Murate, and A. Miyajima. 1997. Oncostatin M and leukemia inhibitory factor do not use the same functional receptor in mice. *Blood*. 90:165–173.
4. Kopf, M., H. Baumann, G. Freer, M. Freudenberg, M. Lamers, T. Kishimoto, R. Zinkernagel, H. Bluethmann, and G. Kohler. 1994. Impaired immune and acute-phase responses in interleukin-6-deficient mice. *Nature*. 368:339–342.
5. Stewart, C.L., P. Kaspar, L.J. Brunet, H. Bhatt, I. Gadi, F. Köntgen, and S.J. Abbondanzo. 1992. Blastocyst implantation depends on maternal expression of leukaemia inhibitory factor. *Nature*. 359:76–79.
6. Masu, Y., E. Wolf, B. Holtmann, M. Sendtner, G. Brem, and H. Thoenen. 1993. Disruption of the CNTF gene results in motor neuron degeneration. *Nature*. 365:27–32.
7. Nandurkar, H.H., L. Robb, D. Tarlinton, L. Barnett, F. Köntgen, and C.G. Begley. 1997. Adult mice with targeted mutation of the interleukin-11 receptor (IL11Rα) display normal hematopoiesis. *Blood*. 90:2148–2159.
8. Robb, L., R. Li, L. Hartley, H.H. Nandurkar, F. Köntgen, and C.G. Begley. 1998. Infertility in female mice lacking the receptor for interleukin 11 is due to a defective uterine response to implantation. *Nat. Med*. 4:303–308.
9. Bernad, A., M. Kopf, R. Kulbacki, N. Weich, G. Koehler, and J.C. Gutierrez-Ramos. 1994. Interleukin-6 is required in vivo for the regulation of stem cells and committed progenitors of the hematopoietic system. *Immunity*. 1:725–731.
10. Ramsay, A.J., A.J. Husband, I.A. Ramshaw, S. Bao, K.I. Matthaei, G. Koehler, and M. Kopf. 1994. The role of interleukin-6 in mucosal IgA antibody responses in vivo. *Science*. 264:561–563.
11. Dalrymple, S.A., L.A. Lucian, R. Slattery, T. McNeil, D.M. Aud, S. Fuchino, F. Lee, and R. Murray. 1995. Interleukin-6-deficient mice are highly susceptible to *Listeria monocytogenes* infection: correlation with inefficient neutrophilia. *Infect. Immun*. 63:2262–2268.
12. Romani, L., A. Mencacci, E. Cenci, R. Spaccapelo, C. Toniatti, P. Puccetti, F. Bistoni, and V. Poli. 1996. Impaired neutrophil response and $CD4^+$ T helper cell 1 development in interleukin 6–deficient mice infected with *Candida albicans*. *J. Exp. Med*. 183:1345–1355.
13. Suzuki, Y., S. Rani, O. Liesenfeld, T. Kojima, S. Lim, T.A. Nguyen, S.A. Dalrymple, R. Murray, and J.S. Remington. 1997. Impaired resistance to the development of toxoplasmic encephalitis in interleukin-6-deficient mice. *Infect. Immun*. 65:2339–2345.
14. Romano, M., M. Sironi, C. Toniatti, N. Polentarutti, P. Fruscella, P. Ghezzi, R. Faggioni, W. Luini, V. van Hinsbergh, S. Sozzani, et al. 1997. Role of IL-6 and its soluble receptor in induction of chemokines and leukocyte recruitment. *Immunity*. 6:315–325.
15. Fattori, E., M. Cappelletti, P. Costa, C. Sellitto, L. Cantoni, M. Carelli, R. Faggioni, G. Fantuzzi, P. Ghezzi, and V. Poli. 1994. Defective inflammatory response in interleukin 6–deficient mice. *J. Exp. Med*. 180:1243–1250.
16. Cressman, D.E., L.E. Greenbaum, R.A. De Angelis, G. Ciliberto, E.E. Furth, V. Poli, and R. Taub. 1996. Liver failure and defective hepatocyte regeneration in interleukin-6-deficient mice. *Science*. 274:1379–1383.
17. Chai, Z., S. Gatti, C. Toniatti, V. Poli, and T. Bartfai. 1996. Interleukin (IL)-6 gene expression in the central nervous system is necessary for fever response to lipopolysaccharide or IL-1β: a study on IL-6–deficient mice. *J. Exp. Med*. 183: 311–316.
18. Klein, M.A., J.C. Moller, L.L. Jones, H. Bluethmann, G.W. Kreutzberg, and G. Raivich. 1997. Impaired neuroglial activation in interleukin-6 deficient mice. *Glia*. 19:227–233.
19. Poli, V., R. Balena, E. Fattori, A. Markatos, M. Yamamoto, H. Tanaka, G. Ciliberto, G.A. Rodan, and F. Costantini. 1994. Interleukin-6 deficient mice are protected from bone loss caused by estrogen depletion. *EMBO J*. 13:1189–1196.
20. Escary, J.L., J. Perreau, D. Dumenil, S. Ezine, and P. Brulet. 1993. Leukaemia inhibitory factor is necessary for maintenance of haematopoietic stem cells and thymocyte stimulation. *Nature*. 363:361–364.
21. Ware, C.B., M.C. Horowitz, B.R. Renshaw, J.S. Hunt, D. Liggitt, S.A. Koblar, B.C. Gliniak, H.J. McKenna, T. Papayannopoulou, B. Thoma, et al. 1995. Targeted disruption of the low-affinity leukemia inhibitory factor receptor gene causes placental, skeletal, neural and metabolic defects and results in perinatal death. *Development*. 121:1283–1299.
22. Li, M., M. Sendtner, and A. Smith. 1995. Essential function of LIF receptor in motor neurons. *Nature*. 378:724–727.
23. De Chiara, T.M., R. Vejsada, W.T. Poueymirou, A. Acheson, C. Suri, J.C. Conover, B. Friedman, J. McClain, L. Pan, N. Stahl, et al. 1995. Mice lacking the CNTF receptor, unlike mice lacking CNTF, exhibit profound motor neuron deficits at birth. *Cell*. 83:313–322.
24. Yoshida, K., T. Taga, M. Saito, S. Suematsu, A. Kumanogoh, T. Tanaka, H. Fujiwara, M. Hirata, T. Yamagami, T. Nakahata, et al. 1996. Targeted disruption of gp130, a common signal transducer for the interleukin 6 family of cytokines, leads to myocardial and hematological disorders. *Proc. Natl. Acad. Sci. USA*. 93:407–411.
25. Kawasaki, K., Y.H. Gao, S. Yokose, Y. Kaji, T. Nakamura, T. Suda, K. Yoshida, T. Taga, T. Kishimoto, H. Kataoka, et al. 1997. Osteoclasts are present in gp130-deficient mice. *Endocrinology*. 138:4959–4965.
26. Rajewsky, K., H. Gu, R. Kühn, U.A. Betz, W. Müller, J. Roes, and F. Schwenk. 1996. Conditional gene targeting. *J. Clin. Invest*. 98:600–603.
27. Broudy, V.C., N.L. Lin, N. Fox, T. Taga, M. Saito, and K. Kaushansky. 1996. Thrombopoietin stimulates colony-forming unit-megakaryocyte proliferation and megakaryocyte maturation independently of cytokines that signal through the gp130 receptor subunit. *Blood*. 88:2026–2032.
28. Roes, J., and K. Rajewsky. 1993. Immunoglobulin D (IgD)-deficient mice reveal an auxiliary receptor function for IgD in antigen-mediated recruitment of B cells. *J. Exp. Med*. 177: 45–55.
29. Bachmann, M.F., T.M. Kundig, C.P. Kalberer, H. Hengart-

ner, and R.M. Zinkernagel. 1993. Formalin inactivation of vesicular stomatitis virus impairs T-cell- but not T-help-independent B-cell responses. *J. Virol.* 67:3917–3922.
30. Gu, H., Y.R. Zou, and K. Rajewsky. 1993. Independent control of immunoglobulin switch recombination at individual switch regions evidenced through Cre-loxP-mediated gene targeting. *Cell*. 73:1155–1164.
31. Betz, U.A., C.A. Vosshenrich, K. Rajewsky, and W. Müller. 1996. Bypass of lethality with mosaic mice generated by Cre-loxP-mediated recombination. *Curr. Biol*. 6:1307–1316.
32. Kühn, R., F. Schwenk, M. Aguet, and K. Rajewsky. 1995. Inducible gene targeting in mice. *Science*. 269:1427–1429.
33. Weber, H., D. Valenzuela, G. Lujber, M. Gubler, and C. Weissmann. 1987. Single amino acid changes that render human IFN-alpha 2 biologically active on mouse cells. *EMBO J.* 6:591–598.
34. Lin, Q., C. Dong, and M.D. Cooper. 1998. Impairment of T and B cell development by treatment with a type I interferon. *J. Exp. Med*. 187:79–87.
35. Sendtner, M., R. Gotz, B. Holtmann, J.L. Escary, Y. Masu, P. Carroll, E. Wolf, G. Brem, P. Brulet, and H. Thoenen. 1996. Cryptic physiological trophic support of motoneurons by LIF revealed by double gene targeting of CNTF and LIF. *Curr. Biol*. 6:686–694.
36. Muraguchi, A., T. Hirano, B. Tang, T. Matsuda, Y. Horii, K. Nakajima, and T. Kishimoto. 1988. The essential role of B cell stimulatory factor 2 (BSF-2/IL-6) for the terminal differentiation of B cells. *J. Exp. Med*. 167:332–344.
37. Sadlack, B., R. Kühn, H. Schorle, K. Rajewsky, W. Müller, and I. Horak. 1994. Development and proliferation of lymphocytes in mice deficient for both interleukins-2 and -4. *Eur. J. Immunol*. 24:281–284.
38. Spriggs, M.K., B.H. Koller, T. Sato, P.J. Morrissey, W.C. Fanslow, O. Smithies, R.F. Voice, M.B. Widmer, and C.R. Maliszewski. 1992. Beta 2-microglobulin−, CD8+ T-cell-deficient mice survive inoculation with high doses of vaccinia virus and exhibit altered IgG responses. *Proc. Natl. Acad. Sci. USA*. 89:6070–6074.
39. Huang, S., W. Hendriks, A. Althage, S. Hemmi, H. Bluethmann, R. Kamijo, J. Vilcek, R.M. Zinkernagel, and M. Aguet. 1993. Immune response in mice that lack the interferon-gamma receptor. *Science*. 259:1742–1745.
40. Ramsay, A.J., J. Ruby, and I.A. Ramshaw. 1993. A case for cytokines as effector molecules in the resolution of virus infection. *Immunol. Today*. 14:155–157.
41. Unanue, E.R. 1997. Studies in listeriosis show the strong symbiosis between the innate cellular system and the T-cell response. *Immunol. Rev*. 158:11–25.
42. Benigni, F., G. Fantuzzi, S. Sacco, M. Sironi, P. Pozzi, C.A. Dinarello, J.D. Sipe, V. Poli, M. Cappelletti, G. Paonessa, et al. 1996. Six different cytokines that share GP130 as a receptor subunit, induce serum amyloid A and potentiate the induction of interleukin-6 and the activation of the hypothalamus-pituitary-adrenal axis by interleukin-1. *Blood*. 87:1851–1854.
43. Barres, B.A., R. Schmid, M. Sendnter, and M.C. Raff. 1993. Multiple extracellular signals are required for long-term oligodendrocyte survival. *Development (Camb.)*. 118:283–295.
44. Wallace, P.M., J.F. MacMaster, J.R. Rillema, J. Peng, S.A. Burstein, and M. Shoyab. 1995. Thrombocytopoietic properties of oncostatin M. *Blood*. 86:1310–1315.
45. Suematsu, S., T. Matsuda, K. Aozasa, S. Akira, N. Nakano, S. Ohno, J. Miyazaki, K. Yamamura, T. Hirano, and T. Kishimoto. 1989. IgG1 plasmacytosis in interleukin 6 transgenic mice. *Proc. Natl. Acad. Sci. USA*. 86:7547–7551.
46. Travis, J., and G.S. Salvesen. 1983. Human plasma proteinase inhibitors. *Annu. Rev. Biochem*. 52:655–709.
47. Perlmutter, D.H., and J.A. Pierce. 1989. The alpha 1-antitrypsin gene and emphysema. *Am. J. Physiol*. 257:L147–L162.
48. Cichy, J., S. Rose-John, and J. Travis. 1998. Oncostatin M, leukaemia-inhibitory factor and interleukin 6 trigger different effects on alpha1-proteinase inhibitor synthesis in human lung-derived epithelial cells. *Biochem. J.* 329:335–339.
49. Sallenave, J.M., G.M. Tremblay, J. Gauldie, and C.D. Richards. 1997. Oncostatin M, but not interleukin-6 or leukemia inhibitory factor, stimulates expression of alpha1-proteinase inhibitor in A549 human alveolar epithelial cells. *J. Interferon Cytokine Res.* 17:337–346.